Published in final edited form as:
IEEE Trans Biomed Eng. 2014 June ; 61(6): 1660–1667. doi:10.1109/TBME.2013.2297332.

Noninvasive Imaging of the High Frequency Brain Activity in Focal Epilepsy Patients

Yunfeng Lu [Student Member, IEEE],
Department of Biomedical Engineering, University of Minnesota, Minneapolis, MN 55455 USA

Gregory A. Worrell,
Department of Neurology, Mayo Clinic, Rochester, MN 55901 USA

Huishi Clara Zhang,
Department of Biomedical Engineering, University of Minnesota, Minneapolis, MN 55455 USA

Lin Yang,
Department of Biomedical Engineering, University of Minnesota, Minneapolis, MN 55455 USA

Benjamin Brinkmann,
Department of Neurology, Mayo Clinic, Rochester, MN 55901 USA

Cindy Nelson, and
Department of Neurology, Mayo Clinic, Rochester, MN 55901 USA

Bin He [Fellow, IEEE]
Department of Biomedical Engineering and the Institute for Engineering in Medicine, University of Minnesota, Minneapolis, MN 55455 USA (binhe@umn.edu)

Yunfeng Lu: luxxx273@umn.edu

Abstract

High frequency (HF) activity represents a potential biomarker of the epileptogenic zone in epilepsy patients, the removal of which is considered to be crucial for seizure-free surgical outcome. We proposed a high frequency source imaging (HFSI) approach to noninvasively image the brain sources of scalp recorded high frequency EEG activity. Both computer simulation and clinical patient data analysis were performed to investigate the feasibility of using the HFSI approach to image the sources of HF activity from noninvasive scalp EEG recordings. The HF activity was identified from high-density scalp recordings after high-pass filtering the EEG data and the EEG segments with HF activity were concatenated together to form repetitive HF activity. Independent component analysis was utilized to extract the components corresponding to the HF activity. Noninvasive EEG source imaging using realistic geometric boundary element head modeling was then applied to image the sources of the pathological HF brain activity. Five medically intractable focal epilepsy patients were studied and the estimated sources were found to be concordant with the surgical resection or intracranial recordings of the patients. The present study demonstrates, for the first time, that source imaging from the scalp HF activity could help to localize the seizure onset zone (SOZ) and provide a novel noninvasive way of studying the

Correspondence to: Bin He.

epileptic brain in humans. This study also indicates the potential application of studying HF activity in the pre-surgical planning of medically intractable epilepsy patients.

Index Terms

Source imaging; High frequency activity; Epileptogenic zone; Scalp EEG; Epilepsy

I. Introduction

Epilepsy is a chronic neurological disorder affecting over 50 million people in the world. Patients with epilepsy are usually treated with antiepileptic drugs (AEDs) to control their seizures. However, about 30% of the patients do not respond to the medications and their seizures continue despite trying multiple AEDs [1]. Neurostimulation treatments may be performed in some medically resistant epilepsy patients to suppress seizures. However in the close-loop responsive cortical stimulation [2], localizing the epileptogenic zone is important for guiding the implantation of brain stimulation leads. Surgical intervention is a viable option for the medically resistant focal epilepsy when seizures are impacting their quality of life and no AEDs or medical devices are controlling the seizures [3]. Accurate localization of the epileptogenic zone thus plays a critically important role in guiding the resective surgery and in directing brain stimulation.

Despite considerable efforts made so far, it remains challenging to accurately identify the epileptogenic zone for favorable surgical outcome. Intracranial EEG (iEEG) recordings utilizing subdural grids and depth electrodes are still the gold standard of determining the seizure onset zone (SOZ) of epilepsy patients [4]. However, intracranial recording is an invasive procedure and it involves risks such as cerebral hemorrhage and infection. Current clinical practice requires a prolonged recording for up to ten days in order to identify SOZ, which further increases the risks and complications of this procedure. Furthermore, the intracranial recording has limited spatial coverage since only a limited portion of the cortical surface or brain regions can be covered by the intracranial electrodes [5]–[7]. Structural magnetic resonance imaging (MRI) has also been widely used to image the abnormal structural lesions in epilepsy patients. However, the MRI lesion is not the ideal indicator of epileptogenic zone. Some patients may have multiple non-epileptic lesions while structural lesions may not be revealed with MRI in many other patients. Additional information from other modalities is thus much needed to further understand the epilepsy and to better delineate the epileptogenic zone.

High frequency (HF) brain oscillations are the recorded electrical activity ranging from 30 Hz to 500 Hz, and include gamma, ripple and fast ripple activity [8]. Since the discovery of HF activity in epilepsy patients, many studies have suggested that HF activity may represent an effective biomarker of epileptogenicity [9]–[13]. Studies have shown that HF activity was strongly correlated to the SOZ, with significantly higher HF occurrence rates and durations inside the SOZ than the non-SOZ area [14], [15]. The HF activity is also highly correlated with the follow-up outcome of epilepsy surgery [16], [17]. Studies have shown that the

complete removal of brain areas with HF activity was more likely to achieve a favorable surgical outcome in the epilepsy surgery [18], [19].

EEG/MEG are the noninvasive recording of electrophysiological brain activity and they have been widely used in research labs and clinical centers to help study functioning brain activity and pathological brain abnormalities [7], [20]–[43]. EEG has been routinely recorded in epilepsy centers to identify interictal activity or seizure activity to diagnose and classify epilepsy. Recent studies have also shown that HF activity can be recorded from scalp EEG in both children and adult epilepsy patients [44], [45]. HF activity on scalp EEGs including gamma and ripples were frequently associated with spikes and their occurrences were much higher within than outside of the seizure onset zone [45]. Since the HF activity can be recorded in scalp EEGs, studies estimating the underlying sources of HF activity are desirable to further investigate the feasibility of noninvasively localizing epileptogenic zone.

In the present study, we utilized the noninvasive EEG source imaging approach to image the sources of HF activity recorded by the scalp EEG. HF activity was obtained from non-REM sleep stage of focal epilepsy patients and independent component analysis was used to extract the HF components for source imaging. The estimated sources for HF activity were then quantitatively compared with the surgically resected region and intracranial recordings of the patients.

II. Methods

A. High frequency source imaging

The high frequency source imaging (HFSI) approach consists of concatenating the scalp recorded HF activity and imaging the high frequency components using the EEG source imaging. The scalp HF activity was obtained by reviewing the interictal data of the non-REM sleep EEG recording. The EEG data were high-pass filtered at 30Hz and the HF activity was identified as the activity with at least 3 consecutive oscillations.

The scalp EEG can be represented by modeling the brain electrical sources and the volume conduction effects. The general problem can be written in Equation (1).

$$\Phi = A(R, Q)S \quad (1)$$

The Nm-by-Nt matrix Φ is the electrical potential measured on the scalp, the Nm-by-3Ns matrix $A(R,Q)$ is the transfer matrix (or lead-field matrix), the Ns-by-1 vector R is the location of sources, the Ns-by-3 matrix Q is the orientation of sources, and the Ns-by-3Nt matrix S is the activity of brain sources. Nm is the number of EEG measurement on the scalp, Nt is the number of recorded samples in EEG, and Ns is the dimension of EEG source locations in source domain. The brain sources are modeled as the dipolar current sources located in the 3D brain and the transfer matrix is calculated from the boundary element method (BEM) head model [20], [46].

Since the HF activities are small oscillations and they cannot be averaged, independent component analysis (ICA) was utilized to extract the HF activity. The spatial-temporal EEG

activity can be represented by multiple independent components using ICA as in Equation (2) [32], [47], [48].

$$\Phi = \mathrm{WMT} = \sum_{i=1}^{N_C} w_i M_i T_i \quad (2)$$

where Φ is the recorded scalp EEG, N_C is the number of independent components, w_i is the i^{th} weighting element, M_i and T_i represent the spatial map and temporal activation of i^{th} component, respectively. Each component stands for an independent brain activity with spatial map and temporal activation. The components corresponding to the HF activity can be selected according to the repetitive appearance of HF activity in the component temporal activation. The brain source could then be estimated by solving the inverse problem of the spatial maps of HF components [32]. Specifically, the source reconstruction for each HF component $\hat{S}_i$ will be obtained from its spatial map M_i, and the overall brain source S could then be obtained by combining the HF component sources in the source domain as $\sum_{i=1}^{N_S} w_i \hat{S}_i \hat{T}_i$, where $\hat{S}_i$ is the source of i^{th} HF component and $\hat{T}_i$ is the HF activity of i^{th} component. The estimated source S is thus the integrated result of all the identified HF component sources and it is the same as the individual component source when there is only one identified HF component. Varieties of source models and source imaging methods can be applied to solve the above inverse problem, and here we utilized the distributed current density source model and sLORETA weighted minimum norm estimation (SWARM) to estimate the brain sources [49]. The patient-specific BEM head models were built from the pre-operative structural MR images of the patients. The volume conduction head modeling included three layers (scalp, skull and brain) and their conductivity values were set as 0.33 S/m, 0.0165 S/m and 0.33 S/m, respectively [50], [51].

B. Computer simulation of imaging high frequency activity

A series of computer simulations were performed to study the feasibility of imaging HF activity from the scalp EEG. Dipolar sources were simulated in the cortical structures and the simulated dipoles had random orientations. A standard head volume conduction model, built from MRI images of a human subject, was used to compute the forward problem and the scalp EEG with 76 channels were generated according to the source waveforms. Gaussian white noise was added to the scalp EEG signals to simulate noise contaminated measurements. In order to simulate the noisy conditions in EEG, the generated HF activity on scalp EEG is only slightly larger than the added noise in the EEG channels. We defined the signal-to-noise ratio (SNR) as the root-mean-square amplitude ratio of the signal and noise in the channel, which has the most dominant HF activity. A thousand trials with mean SNR 1.32 and standard deviation 0.39 were simulated to investigate the feasibility of studying HF activity. The HF activity of dipolar sources was simulated as the sinusoidal oscillation with the frequency at 40 Hz and the duration of the activity was set as 100 milliseconds. Background activity with 400 milliseconds in length was also simulated in addition to the HF activity, which leads to 500 milliseconds data for each data segment. Twenty data segments (10 seconds in total) were generated for each simulated dipolar

source and the HF activity together with background activity was used to estimate the source location and source orientation. Localization error (LE) was used to assess the source localization performance by calculating the distance between the location of maximal estimated source and the location of simulated target source. The computer simulation was carried out in 1000 trials and each trial consisted of a dipolar source with random location and orientation.

C. Patient Data Acquisition and Analysis Protocol

The schematic diagram of patient data study is shown in Fig. 1. Five medically intractable focal epilepsy patients were studied and the study protocol was approved by the Institutional Review Boards of the University of Minnesota and the Mayo Clinic. Four patients underwent resective surgery (not spare procedure) and they had surgical outcome follow-up one year after the surgery. Two patients had intracranial recordings available and the seizure onset zones (SOZs) were identified for the patients by experienced epileptologists. All the patients had pre-operative long term EEG monitoring and pre-operative structural magnetic resonance imaging (MRI) scans. The clinical information of the patients is shown in Table 1.

The pre-operative scalp EEG was recorded in the long term video monitoring system with 76 electrodes placed according to the modified international 10-10 montage. The EEG data were filtered with a low-pass filter at 200 Hz and sampled at 500 Hz. The non-REM sleep EEG was then high-pass filtered above 30 Hz and displayed at expanded time-scale to mark the HF activity [45]. The EEG segments containing HF activity were then concatenated together for independent component analysis. The pre-operative and post-operative MRI images (voxel size: 0.9375* 0.9375* 1.0 mm3) of the patients were acquired from a 1.5 Tesla or 3 Tesla GE Signa scanner (General Electric Medical Systems, Milwaukee, WI).

The source imaging results of high frequency activity were compared with the results of interictal spikes. The spikes were identified as these brief interictal discharges that had abrupt polarity changes from the background EEG. The dominant interictal spikes with similar morphology and topography were selected from each of the studied patients. The number of studied interictal spikes was the same as the number of studied HF activity and the interictal spikes were averaged according to their global field power (GFP) peak for further analysis. The source analysis of the interictal spikes was then performed by solving the inverse problem at the peak timing of the averaged spikes. Same as in estimating the HF activity sources, the SWARM source reconstruction algorithm was utilized to estimate the sources of interictal spikes.

D. Evaluation of imaging results in patients

The estimated sources for HF activity in patients were evaluated by comparing with the surgical resection and intracranial recordings in the same patients. The source location of HF activity was obtained by finding the strength maximum of the estimated source distribution. The surgically resected area was segmented from the post-operative MRI images of the patients. The SOZ was determined from the intracranial recording. Four patients had surgical resection and all of them were rendered seizure free within at least one year follow-

up after the surgery. The localization error, which was defined as the distance from the maximal estimated EEG source to the border of surgically resected regions or to the SOZ of the intracranial recording, was used to quantify the performance of HF source imaging in the epilepsy patients. Two patients had intracranial recording available, and the estimated sources were compared with the seizure onset zone that was marked on the intracranial recording electrodes.

III. Results

A. Computer simulation

The computer simulation results of imaging HF activity are shown in Fig. 2. One thousand trials were simulated and each trial included a dipolar source with random location and orientation located in the cortex. Fig. 2a shows the simulation settings of one simulated dipolar source. The location of the dipolar source is highlighted with the green dot and it is located in the left frontal lobe. Fig. 2b shows the simulated scalp EEG from the dipolar source based on the forward computation of the standard head modeling. Fig. 2c shows the source imaging results and the independent components of the high frequency activity. The estimated source is in the left frontal lobe and it is co-localized with the simulated source in frontal head region. The source imaging results from the 1000 trials are shown in Fig. 2d. The localization error is used to evaluate the performance in the computer simulation. The simulated trials are categorized into four groups (frontal, occipital, parietal and temporal groups) according to the locations of simulated dipoles. The results show that the mean localization errors are around 1 cm for all the groups with the smaller localization errors in frontal and parietal groups.

B. Imaging the high frequency activity

Patient 1 was a medically intractable patient with right temporal lobe epilepsy and the imaging results in the patient are shown in Fig. 3. Fig. 3a displays the wide-band raw EEG activity (left panel) and high-pass filtered EEG (right panel). The non-REM sleep EEG showed interictal spikes in the right hemisphere. Fig. 3b shows the independent component corresponding to the HF activity. The time activation of the component shows repetitive HF activity and the spatial map indicates that the activity is in the right temporal region. The source imaging result of the HF activity is displayed together with the cortex of the patient in Fig. 3c. This patient had the right temporal lobectomy and the resected brain region is highlighted with the red circle in Fig. 3d. The maximum of the estimated source is located in the right temporal lobe, which is concordant with the surgical resection of the patient.

The imaging results of Patient 2 are shown in Fig. 4. This patient had left temporal lobe epilepsy and was 33 years old during the epilepsy treatment. The non-REM sleep raw EEG show spikes in the left hemisphere and the high-pass filtered EEG show high frequency activity in left temporal head regions (Fig. 4a). Fig. 4b shows the independent component of the HF activity, which has repetitive HF time course and the spatial map is focused in left temporal region. The source imaging result of the HF activity is shown in Fig. 4c and the source maximum is in the left temporal lobe of the patient. This patient had left temporal lobectomy as demonstrated in Fig. 4d.

Patient 5 was a 26-year-old female epilepsy patient with left temporal seizures. The non-REM sleep EEG shows interictal spikes and the high-pass filtered EEG shows high frequency activity in the left hemisphere (Fig. 5a). Fig. 5b shows the independent component of the HF activity, which has repetitive HF time course and the spatial map is focused in left temporal region. The source imaging result of the patient is in the left temporal lobe region and it is concordant with the seizure onset zone of intracranial recording as shown in Fig. 5d.

The source imaging results of all five patients are summarized in Fig. 7. The estimated sources of the patients were evaluated with surgical resection and intracranial recordings. In three out of the four patients with surgical treatment, the estimated source maxima were located inside the surgically resected regions. The estimated source in the remaining patient was close to the resection boundary. In the two patients with intracranial recording available, the estimated sources were overlapped with the SOZ determined from intracranial recordings. In addition to the source analysis of high frequency activity, we also analyzed the sources of interictal spikes in the same group of studied patients.

C. High frequency activity and interictal spikes

The source imaging results of high frequency activity were compared with the results of interictal spikes. Fig. 6 shows the source imaging results of HF activity and interictal spike in Patient 4. Fig. 6a shows the results of HF activity as displayed with intracranial recording electrodes and pre-operative MRI images of the patient. The imaged source of HF activity is located in the left parietal lobe, and it is concordant with the SOZ of intracranial recording and the surgical resection as highlighted in Fig. 6c. The source imaging result from conventional interictal EEG spike is shown in Fig. 6b. The spike result is in medial area and it is slightly shifted from the SOZ as determined from intracranial EEG and surgical resection. This result suggests that the HF activity source imaging could more accurately image the location of epileptogenic sources than the spike analysis. The localization of HF activity and spikes are also quantitatively compared in the four patients (Patient 1, Patient 2, Patient 3, and Patient 4) who had surgical resection available and in the two patients (Patient 4 and Patient 5) who had intracranial recording available. The averaged localization error to the surgical resection is 0.25 cm in HF activity and 0.53 cm in the spike results (Fig. 7a). The averaged localization error to the seizure onset zone of intracranial recording is 1.2 cm in HF activity while it is over 2 cm in the spike results (Fig. 7b). The above results show that the HF activity is more effective in imaging the epileptogenic zone than the interictal spike as compared with the SOZ of intracranial recording and the surgical resection.

IV. Discussion

In the present study, we imaged the brain sources of scalp high frequency activity in five medically intractable focal epilepsy patients. The estimated brain sources of HF activity were concordant with the locations of surgical resection and SOZ determined from intracranial recordings. The imaging of HF activity also showed improved performance in localizing epileptogenic zone as compared with the traditional source analysis of interictal spikes. This study demonstrates that source imaging of the scalp HF activity may represent a

new noninvasive way of identifying the epileptogenic zone for the pre-surgical planning of epilepsy treatment.

High frequency brain oscillations appear to be an effective biomarker of delineating the pathological epileptogenic zone from the normal brain regions [12], [52]. Studies have shown that brain areas with high frequency (HF) activity greatly overlapped with the SOZ and the HF activity is more likely to occur within the SOZ than in other regions. Retrospective studies also showed that there is a strong association between seizure-free outcome and removal of HF generating regions during the surgical treatment [16]. Another reason to suggest HF activity as an effective biomarker is that HF activity is useful in revealing epileptogenic zone rather than indicating the non-specific pathological MRI lesions [53], [54]. This property ensures that HF activity could be used to identify the epileptogenic zone in MRI-negative patients and to exclude the non-epileptic MRI abnormalities in patients with multiple lesions. Since the report of successful recording of HF brain oscillation in epilepsy patients, various studies have demonstrated the usefulness of HF activity in the pre-surgical planning of epilepsy treatment. Recent studies of epilepsy patients also reported the recording of HF brain oscillations in scalp EEGs, which suggested the importance of noninvasive study on the HF activity for potential clinical application [44], [45].

EEG/MEG source imaging has been previously used to analyze the functioning brain response in normal subjects and to study the pathological brain activity in epilepsy patients [7], [30], [34], [55]–[58]. The advancement in source imaging techniques has enabled the feasibility of studying the underlying brain sources from the noninvasive recording of electromagnetic activity. Scanning methods such as multiple signal classification and spatial filtering approaches has been utilized to probe the brain electrical sources from noninvasive recordings [30], [40], [59]–[62]. Source imaging methods for current density models were also developed to image the active brain sources with certain distribution [63]–[65]. Previous source imaging studies of epilepsy patients have been mainly focused on the spikes during the interictal periods. Considering the effectiveness of high frequency brain activity in characterizing the epileptogenic zone, it remains important to study the cortical brain sources corresponding to the scalp high frequency activity. In this study, the scalp high frequency activity was successfully imaged and the estimated brain sources were concordant with the seizure onset zone as referenced from surgical resection and intracranial recording of the patients.

An important issue in the EEG source analysis of epilepsy patients is to record the desired epileptic events and to image the events with high spatial and temporal resolution. In this study, the scalp electrophysiological activity of epilepsy patients was recorded using the long-term video EEG monitoring system. The long-term monitoring enabled the recording of EEG activity during the sleep stage of the patients while the head moving artifacts could be minimized [45]. The sampling frequency of the recording was set at 500 Hz to capture the high frequency activity above 30 Hz of the scalp EEG. Studies have shown that the source localization accuracy could be improved by utilizing the dense-array EEG recording system [23], [30]. High-density EEG recording with 76 electrodes were utilized in this study to overcome the limited spatial sampling of 19 or 21 channels as in the routine clinical

settings. The patient-specific realistic geometric BEM head modeling was used in the study to further minimize the localization error that is caused by the inaccuracy of volume conduction modeling [20], [46], [66]. In the present study, the scalp recorded HF activity was processed with independent component analysis to extract the HF components. The number of selected ICs varies among the patients and it ranges from one to three components in the studied patients. When more than one IC is identified, the HF sources for each of the identified IC are estimated and the source results are obtained by combining the component sources in the source domain. HF activity was obtained during the non-REM sleep EEG of the patients in order to minimize the recording noise. Future studies incorporating advance techniques to study the HF activity in other routine EEG recordings such as during less frequent spikes or during ictal events may be necessary to further investigate the high frequency activity in more noisy conditions and improve the clinical application. All patients in the current study had partial epilepsy with single epileptic focus, and studies including more patients and more complicated patients such as patients with multiple foci would be beneficial to expand the analysis in more general epilepsy cases. Future studies comparing the scalp HF activity with invasive high frequency activity may also be necessary to further understand the epileptic activity and enhance the application.

Despite the great efforts of many studies in imaging the epileptogenic zone, it remains a significant challenge to accurately identify the abnormal brain regions for a successful surgical treatment. Various imaging modalities have been used to image the epileptogenic zone in medically intractable epilepsy patients. Single-photon emission computed tomography (SPECT) and positron emission tomography (PET) have been applied to study the perfusion and metabolism of epileptic brain. Functional MRI (fMRI) was also utilized to study the BOLD response under resting state of epilepsy patients. Recent studies have shown that multimodal neuroimaging combining the EEG and fMRI could achieve improved performance by integrating the high temporal resolution of EEG and high spatial resolution of fMRI [48], [67]–[71]. Studies also revealed the strong spatial correlation between the task-related fMRI activation and gamma activity of intracranial EEG in the same epilepsy patients [72]. Advanced algorithms and techniques have been previously developed to help on the diagnosis and treatment of epilepsy [73]–[85]. Future studies investigating the feasibility of integrating high frequency EEG activity and spontaneous fMRI is still necessary to further develop advanced multimodal neuroimaging techniques for the clinical application in epilepsy patient management.

In conclusion, we proposed the high frequency source imaging method to image the high frequency brain activity from scalp EEGs of epilepsy patients. A series of computer simulations have been performed to test the feasibility of imaging the dipolar sources with high frequency source activity. The proposed method has been evaluated in five medically intractable epilepsy patients and it successfully imaged the underlying sources of scalp high frequency activity as compared with the surgical resection and intracranial recording of the patients. The present study demonstrates, for the first time, the feasibility of noninvasively imaging scalp high frequency activity in the epilepsy patients. It also indicates its potential application as a novel noninvasive way of localizing the epileptogenic zone and in aiding the pre-surgical planning of epilepsy treatment.

Acknowledgments

This work was supported in part by NIH EB006433, EB007920, NSF CBET-0933067, and a grant from the Minnesota Partnership for Biotechnology and Medical Genomics. Y. Lu was supported in part by a Doctoral Dissertation Fellowship from the University of Minnesota.

References

1. Cascino GD. Commentary: how has neuroimaging improved patient care? Epilepsia. 1994; 35(6):S103–S107. [PubMed: 8206009]
2. Morrell MJ. Responsive cortical stimulation for the treatment of medically intractable partial epilepsy. Neurology. 2011; 77(13):1295–1304. [PubMed: 21917777]
3. Engel, J, Jr.. Approaches to localization of the epileptogenic lesion. In: Engel, J., Jr., editor. Surgical Treatment of the Epilepsies. New York: Raven Press; 1987. p. 75-95.
4. Rosenow F, Lüders H. Presurgical evaluation of epilepsy. Brain. 2001; 124(9):1683. [PubMed: 11522572]
5. Wilke C, Van Drongelen W, Kohrman M, He B. Neocortical seizure foci localization by means of a directed transfer function method. Epilepsia. Oct; 2010 51(4):564–572. [PubMed: 19817817]
6. Wilke C, Worrell G, He B. Graph analysis of epileptogenic networks in human partial epilepsy. Epilepsia. 2011; 52(1):84–93. [PubMed: 21126244]
7. Lai Y, Zhang X, van Drongelen W, Korhman M, Hecox K, Ni Y, He B. Noninvasive cortical imaging of epileptiform activities from interictal spikes in pediatric patients. Neuroimage. Jan; 2011 54(1):244–252. [PubMed: 20643212]
8. Engel J Jr. da Silva FL. High-frequency oscillations - Where we are and where we need to go. Prog. Neurobiol. 2012; 98(3):316–318. [PubMed: 22342736]
9. Bragin A, Engel J, Wilson CL, Fried I, Buzsáki G. High-frequency oscillations in human brain. Hippocampus. 1999; 9(2):137–142. [PubMed: 10226774]
10. Jirsch J, Urrestarazu E, LeVan P, Olivier A, Dubeau F, Gotman J. High-frequency oscillations during human focal seizures. Brain. 2006; 129(6):1593–1608. [PubMed: 16632553]
11. Worrell GA, Gardner AB, Stead SM, Hu S, Goerss S, Cascino GJ, Meyer FB, Marsh R, Litt B. High-frequency oscillations in human temporal lobe: simultaneous microwire and clinical macroelectrode recordings. Brain. 2008; 131(4):928–937. [PubMed: 18263625]
12. Jacobs J, Staba R, Asano E, Otsubo H, Wu JY, Zijlmans M, Mohamed I, Kahane P, Dubeau F, Navarro V, Gotman J. High-frequency oscillations (HFOs) in clinical epilepsy. Prog. Neurobiol. 2012; 98(3):302–315. [PubMed: 22480752]
13. Worrell GA, Jerbi K, Kobayashi K, Lina JM, Zelmann R, Le Van Quyen M. Recording and analysis techniques for high-frequency oscillations. Prog. Neurobiol. 2012; 98(3):265–278. [PubMed: 22420981]
14. Crépon B, Navarro V, Hasboun D, Clemenceau S, Martinerie J, Baulac M, Adam C, Le Van Quyen M. Mapping interictal oscillations greater than 200 Hz recorded with intracranial macroelectrodes in human epilepsy. Brain. 2010; 133(1):33–45. [PubMed: 19920064]
15. Jacobs J, LeVan P, Chander R, Hall J, Dubeau F, Gotman J. Interictal high-frequency oscillations (80–500 Hz) are an indicator of seizure onset areas independent of spikes in the human epileptic brain. Epilepsia. 2008; 49(11):1893–1907. [PubMed: 18479382]
16. Ochi A, Otsubo H, Donner EJ, Elliott I, Iwata R, Funaki T, Akizuki Y, Akiyama T, Imai K, Rutka JT. Dynamic Changes of Ictal High-Frequency Oscillations in Neocortical Epilepsy: Using Multiple Band Frequency Analysis. Epilepsia. 2007; 48(2):286–296. [PubMed: 17295622]
17. Akiyama T, Chan DW, Go CY, Ochi A, Elliott IM, Donner EJ, Weiss SK, Snead III OC, Rutka JT, Drake JM. Topographic movie of intracranial ictal high-frequency oscillations with seizure semiology: Epileptic network in Jacksonian seizures. Epilepsia. 2011; 52(1):75–83. [PubMed: 21070217]
18. Wu J, Sankar R, Lerner J, Matsumoto J, Vinters H, Mathern G. Removing interictal fast ripples on electrocorticography linked with seizure freedom in children. Neurology. 2010; 75(19):1686–1694. [PubMed: 20926787]

19. Jacobs J, Zijlmans M, Zelmann R, Chatillon C, Hall J, Olivier A, Dubeau F, Gotman J. High-frequency electroencephalographic oscillations correlate with outcome of epilepsy surgery. Ann. Neurol. 2010; 67(2):209–220. [PubMed: 20225281]
20. He B, Musha T, Okamoto Y, Homma S, Nakajima Y, Sato T. Electric dipole tracing in the brain by means of the boundary element method and its accuracy. IEEE Trans. Biomed. Eng. Jun; 1987 34(6):406–414. [PubMed: 3610187]
21. Sekihara K, Nagarajan SS, Poeppel D, Marantz A, Miyashita Y. Reconstructing spatio-temporal activities of neural sources using an MEG vector beamformer technique. IEEE Trans. Biomed. Eng. Jul; 2001 48(7):760–771. [PubMed: 11442288]
22. Baillet S, Mosher JC, Leahy RM. Electromagnetic brain mapping. Signal Processing Magazine, IEEE. 2001; 18(6):14–30.
23. Lantz G, Grave de Peralta R, Spinelli L, Seeck M, Michel CM. Epileptic source localization with high density EEG: how many electrodes are needed? Clin. Neurophysiol. 2003; 114(1):63–69. [PubMed: 12495765]
24. Zhang X, van Drongelen W, Hecox KE, Towle VL, Frim DM, McGee AB, He B. High-resolution EEG: Cortical potential imaging of interictal spikes. Clin. Neurophysiol. 2003; 114(10):1963–1973. [PubMed: 14499758]
25. Michel CM, Lantz G, Spinelli L, de Peralta RG, Landis T, Seeck M. 128-channel EEG source imaging in epilepsy: clinical yield and localization precision. J. Clin. Neurophysiol. Mar; 2004 21(2):71–83. [PubMed: 15284597]
26. Ebersole JS, Hawes-Ebersole S. Clinical application of dipole models in the localization of epileptiform activity. Journal of Clinical Neurophysiology. 2007; 24(2):120–129. [PubMed: 17414967]
27. Ding L, Worrell GA, Lagerlund TD, He B. Ictal source analysis: localization and imaging of causal interactions in humans. Neuroimage. Jan; 2007 34(2):575–586. [PubMed: 17112748]
28. Guggisberg AG, Kirsch HE, Mantle MM, Barbaro NM, Nagarajan SS. Fast oscillations associated with interictal spikes localize the epileptogenic zone in patients with partial epilepsy. Neuroimage. 2008; 39(2):661–668. [PubMed: 17977022]
29. He B, Yang L, Wilke C, Yuan H. Electrophysiological Imaging of Brain Activity and Connectivity - Challenges and Opportunities. IEEE Trans. Biomed. Eng. 2011; 58(7):1918–31. [PubMed: 21478071]
30. Lu Y, Yang L, Worrell GA, He B. Seizure source imaging by means of FINE spatio-temporal dipole localization and directed transfer function in partial epilepsy patients. Clinical Neurophysiology. 2012; 123(7):1275–1283. [PubMed: 22172768]
31. Lu Y, Yang L, Worrell GA, Brinkmann B, Nelson C, He B. Dynamic imaging of seizure activity in pediatric epilepsy patients. Clinical Neurophysiology. 2012
32. Yang L, Wilke C, Brinkmann B, Worrell GA, He B. Dynamic imaging of ictal oscillations using non-invasive high-resolution EEG. Neuroimage. 2011; 56(4):1908–1917. [PubMed: 21453776]
33. Yang L, Worrell GA, Nelson C, Brinkmann B, He B. Spectral and spatial shifts of post-ictal slow waves in temporal lobe seizures. Brain. 2012; 135(10):3134–3143. [PubMed: 22923634]
34. He, B.; Ding, L. Electrophysiological mapping and neuroimaging. In: He, B., editor. Neural Engineering. 2013.
35. He B, Dai Y, Astolfi L, Babiloni F, Yuan H, Yang L. < i> eConnectome: A MATLAB toolbox for mapping and imaging of brain functional connectivity. J. Neurosci. Methods. 2011; 2:261–269. [PubMed: 21130115]
36. Wilke C, Ding L, He B. Estimation of time-varying connectivity patterns through the use of an adaptive directed transfer function. IEEE Trans. Biomed. Eng. Nov; 2008 55(11):2557–2564. [PubMed: 18990625]
37. Billings S, Zhao Y, Wei H, Sarrigiannis PG. A parametric method to measure time-varying linear and nonlinear causality with Applications to EEG data. 2013
38. Astolfi L, Cincotti F, Babiloni C, Carducci F, Basilisco A, Rossini PM, Salinari S, Mattia D, Cerutti S, Dayan DB. Estimation of the cortical connectivity by high-resolution EEG and structural equation modeling: simulations and application to finger tapping data. IEEE Trans. Biomed. Eng. 2005; 52(5):757–768. [PubMed: 15887525]

39. Astolfi L, Cincotti F, Mattia D, De Vico Fallani F, Tocci A, Colosimo A, Salinari S, Marciani MG, Hesse W, Witte H. Tracking the time-varying cortical connectivity patterns by adaptive multivariate estimators. IEEE Trans. Biomed. Eng. 2008; 55(3):902–913. [PubMed: 18334381]
40. Van Veen BD, Van Drongelen W, Yuchtman M, Suzuki A. Localization of brain electrical activity via linearly constrained minimum variance spatial filtering. IEEE Trans. Biomed. Eng. Sep; 1997 44(9):867–880. [PubMed: 9282479]
41. Bai X, He B. Estimation of number of independent brain electric sources from the scalp EEGs. IEEE Trans. Biomed. Eng. 2006; 53(10):1883–1892. [PubMed: 17019851]
42. Wang Y, He B. A computer simulation study of cortical imaging from scalp potentials. IEEE Trans. Biomed. Eng. Jun; 1998 45(6):724–735. [PubMed: 9609937]
43. He B, Coleman T, Genin GM, Glover G, Hu X, Johnson N, Liu T, Makeig S, Sajda P, Ye K. Grand Challenges in Mapping the Human Brain: NSF Workshop Report. IEEE Trans. Biomed. Eng. 2013; 60(11):2983. [PubMed: 24108705]
44. Kobayashi K, Yoshinaga H, Toda Y, Inoue T, Oka M, Ohtsuka Y. High-frequency oscillations in idiopathic partial epilepsy of childhood. Epilepsia. 2011; 52(10):1812–1819. [PubMed: 21762448]
45. Andrade-Valenca L, Dubeau F, Mari F, Zelmann R, Gotman J. Interictal scalp fast oscillations as a marker of the seizure onset zone. Neurology. 2011; 77(6):524–531. [PubMed: 21753167]
46. Hämäläinen MS, Sarvas J. Realistic conductivity geometry model of the human head for interpretation of neuromagnetic data. IEEE Trans. Biomed. Eng. Feb; 1989 36(2):165–171. [PubMed: 2917762]
47. Delorme A, Makeig S. EEGLAB: an open source toolbox for analysis of single-trial EEG dynamics including independent component analysis. J. Neurosci. Methods. 2004; 134(1):9–21. [PubMed: 15102499]
48. Yang L, Liu Z, He B. EEG-fMRI reciprocal functional neuroimaging. Clin. Neurophysiol. Aug; 2010 121(8):1240–1250. [PubMed: 20378397]
49. Wagner M, Fuchs M, Kastner J. SWARM: sLORETA-weighted accurate minimum norm inverse solutions. Presented at International Congress Series.
50. Lai Y, Van Drongelen W, Ding L, Hecox K, Towle V, Frim D, He B. Estimation of in vivo human brain-to-skull conductivity ratio from simultaneous extra-and intra-cranial electrical potential recordings. Clin. Neurophysiol. 2005; 116(2):456–465. [PubMed: 15661122]
51. Zhang Y, van Drongelen W, He B. Estimation of in vivo brain-to-skull conductivity ratio in humans. Appl. Phys. Lett. 2006; 89(22):223903. [PubMed: 17492058]
52. Worrell G, Gotman J. High-frequency oscillations and other electrophysiological biomarkers of epilepsy: clinical studies. Biomarkers. 2011; 5(5):557–566.
53. Staba RJ, Frighetto L, Behnke EJ, Mathern GW, Fields T, Bragin A, Ogren J, Fried I, Wilson CL, Engel J. Increased fast ripple to ripple ratios correlate with reduced hippocampal volumes and neuron loss in temporal lobe epilepsy patients. Epilepsia. 2007; 48(11):2130–2138. [PubMed: 17662059]
54. Jacobs J, LeVan P, Châtillon C, Olivier A, Dubeau F, Gotman J. High frequency oscillations in intracranial EEGs mark epileptogenicity rather than lesion type. Brain. 2009; 132(4):1022–1037. [PubMed: 19297507]
55. Darvas F, Pantazis D, Kucukaltun-Yildirim E, Leahy RM. Mapping human brain function with MEG and EEG: methods and validation. Neuroimage. 2004; 23(S1):S289–S299. [PubMed: 15501098]
56. Plummer C, Litewka L, Farish S, Harvey A, Cook M. Clinical utility of current-generation dipole modelling of scalp EEG. Clinical Neurophysiology. 2007; 118(11):2344–2361. [PubMed: 17889598]
57. Kaiboriboon K, Nagarajan S, Mantle M, Kirsch HE. Interictal MEG/MSI in intractable mesial temporal lobe epilepsy: spike yield and characterization. Clinical Neurophysiology. 2010; 121(3): 325–331. [PubMed: 20064741]
58. Wang ZI, Jin K, Kakisaka Y, Mosher JC, Bingaman WE, Kotagal P, Burgess RC, Najm IM, Alexopoulos AV. Imag (in) ing seizure propagation: MEG-guided interpretation of epileptic activity from a deep source. Hum. Brain Mapp. 2012

59. Leahy R, Mosher J, Spencer M, Huang M, Lewine J. A study of dipole localization accuracy for MEG and EEG using a human skull phantom. Electroencephalogr. Clin. Neurophysiol. 1998; 107(2):159–173. [PubMed: 9751287]
60. Mosher JC, Leahy RM. Source localization using recursively applied and projected (RAP) MUSIC. IEEE Trans. Signal Proc. Feb; 1999 47(2):332–340.
61. Xu XL, Xu B, He B. An alternative subspace approach to EEG dipole source localization. Phys. Med. Biol. Jan.2004 49(2):327. [PubMed: 15083674]
62. Ding L, Wilke C, Xu B, Xu X, van Drongelen W, Kohrman M, He B. EEG source imaging: correlating source locations and extents with electrocorticography and surgical resections in epilepsy patients. J. Clin. Neurophysiol. Apr; 2007 24(2):130–136. [PubMed: 17414968]
63. Hämäläinen, MS.; Ilmoniemi, RJ. Helsinki Univ.Technol. Helsinki, Finland, Tech.Rep.TKK-F-A: 1984. Interpreting measured magnetic fields of the brain: estimates of current distributions.
64. Dale AM, Liu AK, Fischl BR, Buckner RL, Belliveau JW, Lewine JD, Halgren E. Dynamic Statistical Parametric Mapping: Combining fMRI and MEG for High-Resolution Imaging of Cortical Activity. Neuron. Apr; 2000 26(1):55–67. [PubMed: 10798392]
65. Pascual-Marqui RD. Standardized low-resolution brain electromagnetic tomography (sLORETA): technical details. Methods Find. Exp. Clin. Pharmacol. 2002; 24(Suppl D):5–12. [PubMed: 12575463]
66. Wang G, Worrell G, Yang L, Wilke C, He B. Interictal spike analysis of high-density EEG in patients with partial epilepsy. Clin. Neurophysiol. 2010; 122(6):1098–1105. [PubMed: 21126908]
67. Babiloni F, Cincotti F, Babiloni C, Carducci F, Mattia D, Astolfi L, Basilisco A, Rossini PM, Ding L, Ni Y, Cheng J, Christine K, Sweeney J, He B. Estimation of the cortical functional connectivity with the multimodal integration of high-resolution EEG and fMRI data by directed transfer function. Neuroimage. Jan; 2005 24(1):118–131. [PubMed: 15588603]
68. Pittau F, LeVan P, Moeller F, Gholipour T, Haegelen C, Zelmann R, Dubeau F, Gotman J. Changes preceding interictal epileptic EEG abnormalities: Comparison between EEG/fMRI and intracerebral EEG. Epilepsia. 2011; 52(6):1120–1129. [PubMed: 21671923]
69. He B, Liu Z. Multimodal functional neuroimaging: Integrating functional MRI and EEG/MEG. IEEE Rev. Biomed. Eng. Nov.2008 1:23–40. [PubMed: 20634915]
70. Liu Z, He B. fMRI-EEG integrated cortical source imaging by use of time-variant spatial constraints. Neuroimage. 2008; 39(3):1198–1214. [PubMed: 18036833]
71. Vulliemoz S, Carmichael DW, Rosenkranz K, Diehl B, Rodionov R, Walker MC, McEvoy AW, Lemieux L. Simultaneous intracranial EEG and fMRI of interictal epileptic discharges in humans. Neuroimage. 2011; 54(1):182–190. [PubMed: 20708083]
72. Lachaux J, Fonlupt P, Kahane P, Minotti L, Hoffmann D, Bertrand O, Baciu M. Relationship between task-related gamma oscillations and BOLD signal: New insights from combined fMRI and intracranial EEG. Hum. Brain Mapp. 2007; 28(12):1368–1375. [PubMed: 17274021]
73. Conradsen I, Beniczky S, Hoppe K, Wolf P, Sorensen HB. Automated Algorithm for Generalized Tonic-Clonic Epileptic Seizure Onset Detection Based on sEMG Zero-Crossing Rate. Biomedical Engineering, IEEE Transactions On. 2012; 59(2):579–585.
74. Temko A, Lightbody G, Thomas EM, Boylan GB, Marnane W. Instantaneous measure of EEG channel importance for improved patient-adaptive neonatal seizure detection. Biomedical Engineering, IEEE Transactions On. 2012; 59(3):717–727.
75. Rana P, Lipor J, Lee H, van Drongelen W, Kohrman MH, Van Veen B. Seizure detection using the Phase-Slope Index and multichannel ECoG. Biomedical Engineering, IEEE Transactions On. 2012; 59(4):1125–1134.
76. Yadav R, Swamy M, Agarwal R. Model-based seizure detection for intracranial EEG recordings. Biomedical Engineering, IEEE Transactions On. 2012; 59(5):1419–1428.
77. Yadav R, Shah A, Loeb J, Swamy M, Agarwal R. Morphology-Based Automatic Seizure Detector for Intracerebral EEG Recordings. Biomedical Engineering, IEEE Transactions On. 2012; 59(7): 1871–1881.
78. Sun J, Hong X, Tong S. Phase synchronization analysis of EEG signals: an evaluation based on surrogate tests. Biomedical Engineering, IEEE Transactions On. 2012; 59(8):2254–2263.

79. De Silva A, Sinclair NC, Liley D. Limitations in the Rapid Extraction of Evoked Potentials Using Parametric Modeling. Biomedical Engineering, IEEE Transactions On. 2012; 59(5):1462–1471.

80. Liu Y, De Vos M, Gligorijevic I, Matic V, Li Y, Van Huffel S. Multi-structural signal recovery for biomedical compressive sensing. IEEE Transactions on Biomedical Engineering, accepted. 2013

81. Fukushima M, Yamashita O, Kanemura A, Ishii S, Kawato M, Sato M. A State-Space Modeling Approach for Localization of Focal Current Sources From MEG. Biomedical Engineering, IEEE Transactions On. 2012; 59(6):1561–1571.

82. Wu SC, Swindlehurst AL, Wang PT, Nenadic Z. Efficient dipole parameter estimation in EEG systems with near-ML performance. Biomedical Engineering, IEEE Transactions On. 2012; 59(5): 1339–1348.

83. Wu SC, Swindlehurst AL, Wang PT, Nenadic Z. Projection Versus Prewhitening for EEG Interference Suppression. Biomedical Engineering, IEEE Transactions On. 2012; 59(5):1329–1338.

84. Collier TJ, Kynor DB, Bieszczad J, Audette WE, Kobylarz EJ, Diamond SG. Creation of a Human Head Phantom for Testing of Electroencephalography Equipment and Techniques. Biomedical Engineering, IEEE Transactions On. 2012; 59(9):2628–2634.

85. Wang H, Tang Q, Zheng W. L1-norm-based common spatial patterns. Biomedical Engineering, IEEE Transactions On. 2012; 59(3):653–662.

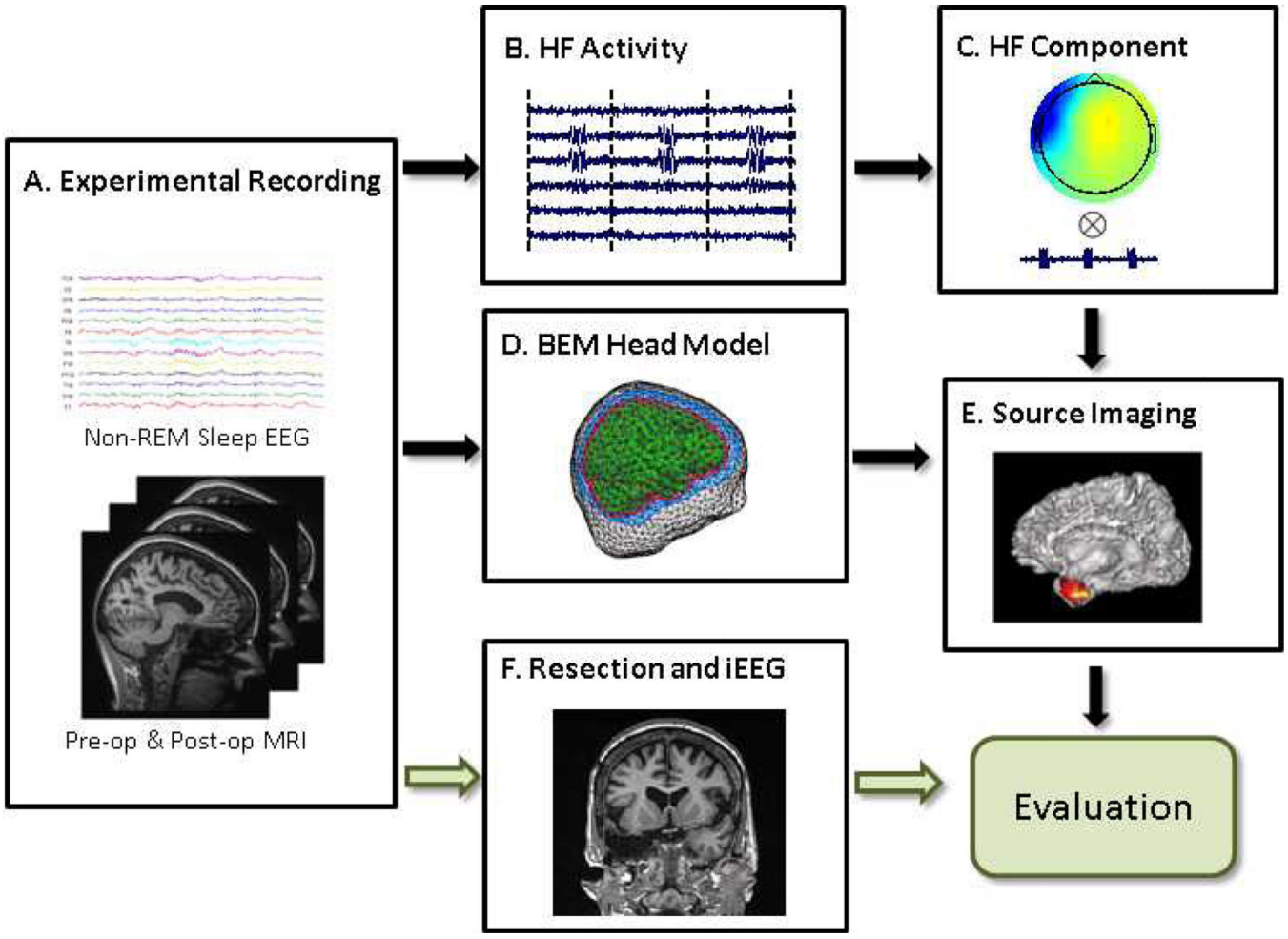

Fig. 1.

Illustration diagram and study design of imaging high frequency (HF) activity. A: Experimental recording including non-REM sleep scalp EEG recording, pre-operative and post-operative MRI scans. B: Concatenated high frequency activity. C: Independent component according to the HF activity. D: Patient-specific boundary element head model. E: Source imaging of the HF activity. F: Surgical resection and intracranial recording of the patient.

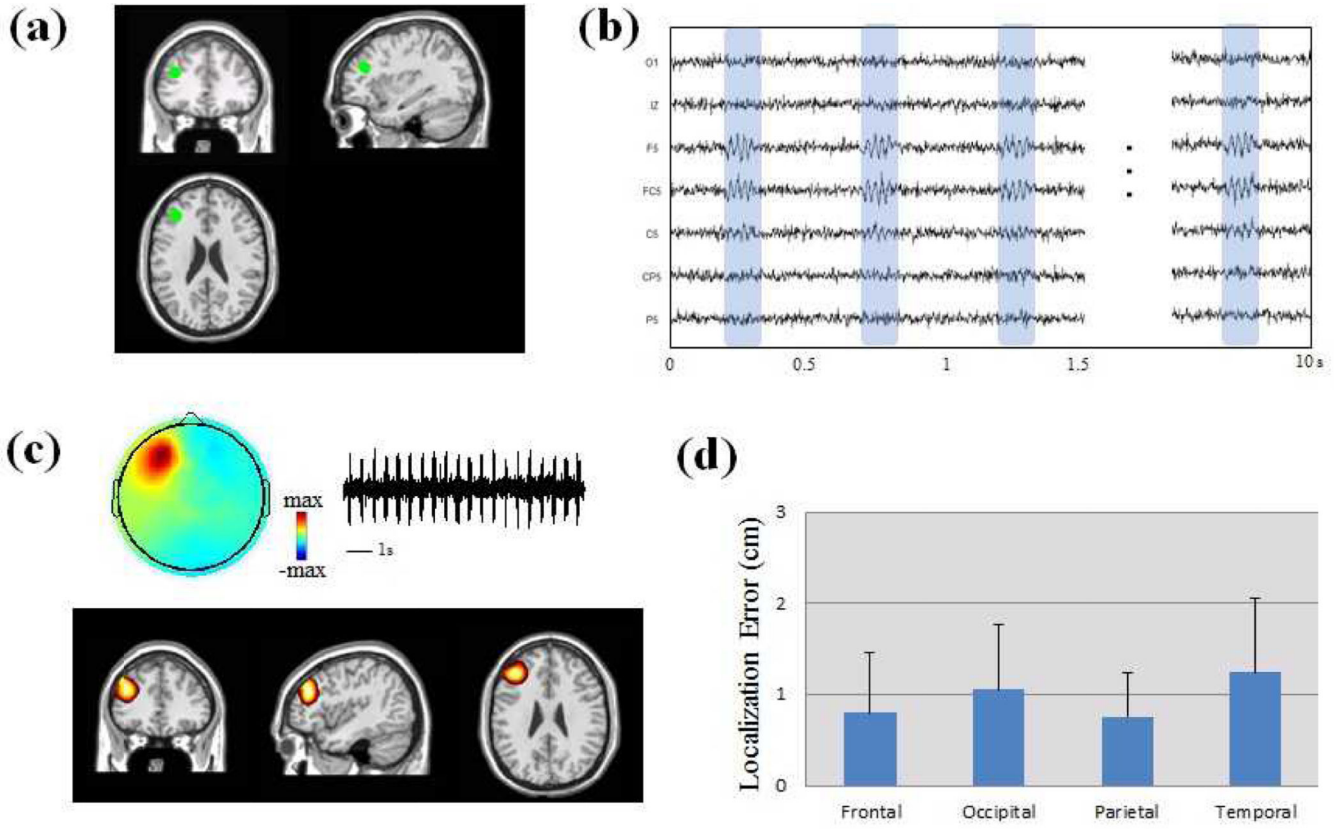

Fig. 2.

Computer simulation of HF activity in a standard head volume conduction model. (a) Location of one simulated dipole source without extent in frontal lobe. (b) Scalp EEG traces generated from the simulated source. (c) Estimated sources and independent component of the HF activity. (d) Localization error (LE) of computer simulation in 1000 trials. The simulated dipoles are categorized in four groups according to the dipole locations (Frontal, Occipital, Parietal and Temporal groups).

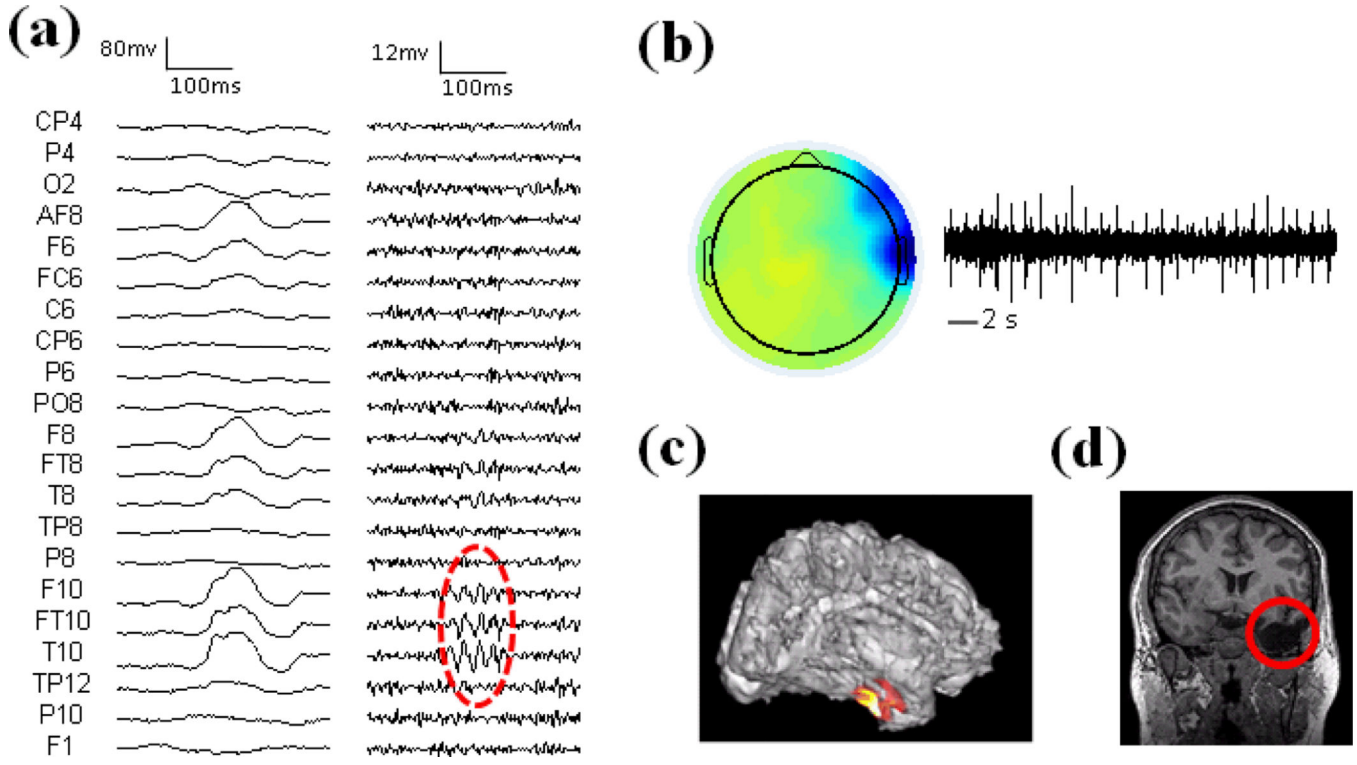

Fig. 3.

Results in Patient 1. (a) Left: Raw EEG; Right: High-pass filtered EEG above 30 Hz. HF activity is marked with red circle. (b) Spatial map and temporal activation of one HF component. (c) Source imaging results of HF activity. (d) Surgical resection is highlighted in red.

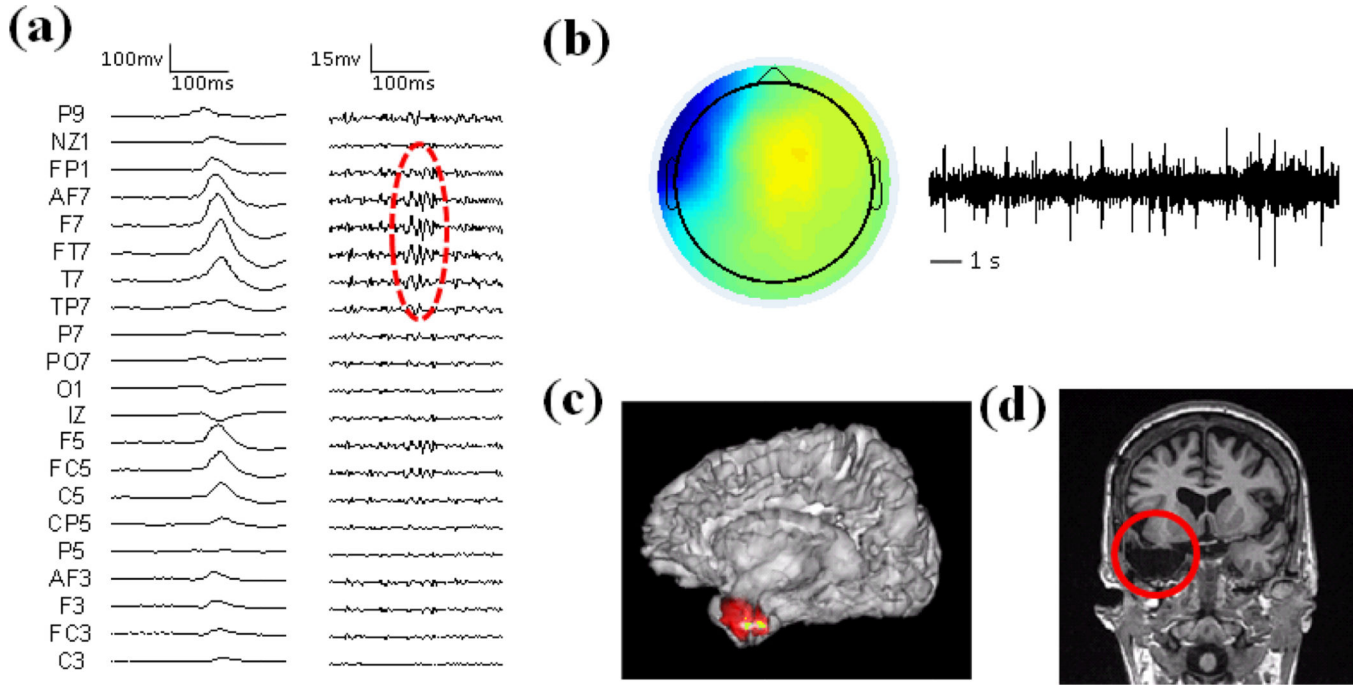

Fig. 4.

Results in Patient 2. (a) Left: Raw EEG; Right: High-pass filtered EEG above 30 Hz. HF activity is marked with red circle. (b) Spatial map and temporal activation of one HF component. (c) Source imaging results of HF activity. (d) Surgical resection is highlighted in red.

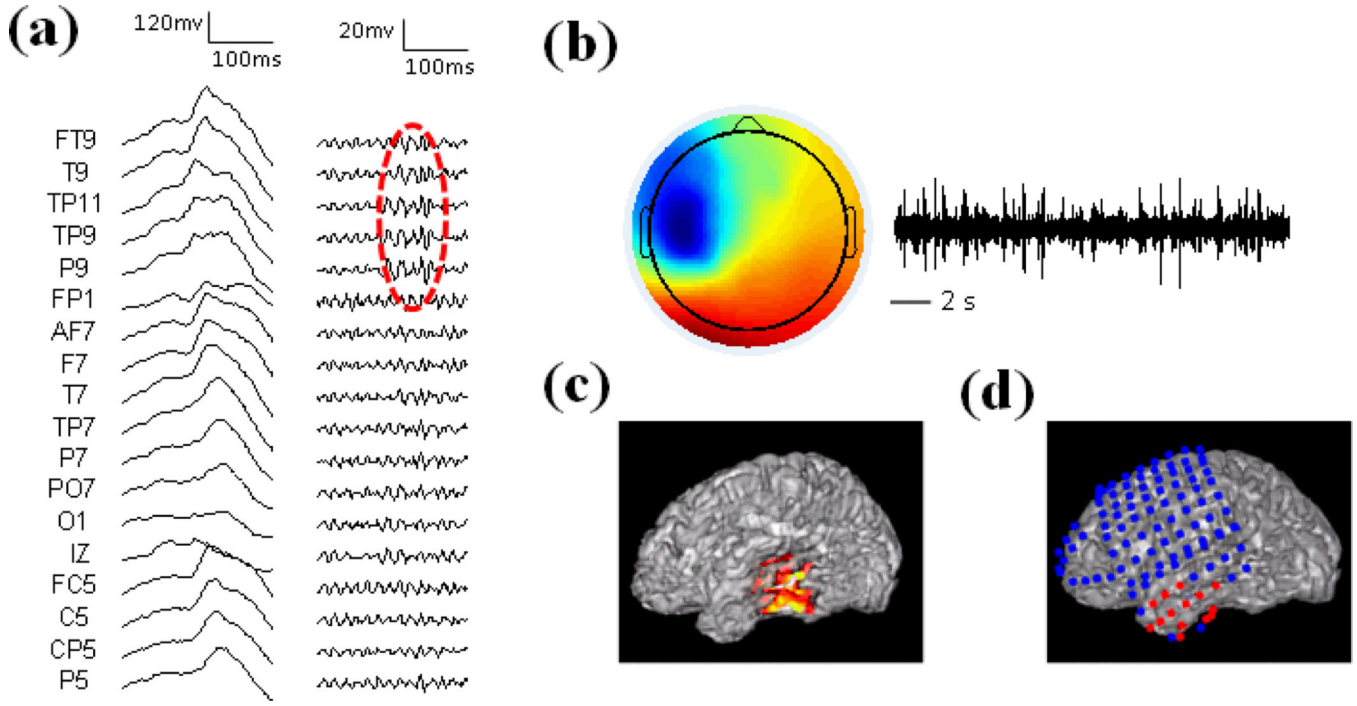

Fig. 5.

Results in Patient 5. (a) Left: Raw EEG; Right: High-pass filtered EEG above 30 Hz. HF activity is marked with red circle. (b) Spatial map and temporal activation of one HF component. (c) Source imaging results of HF activity. (d) Seizure onset zone of intracranial recording is highlighted with red dots.

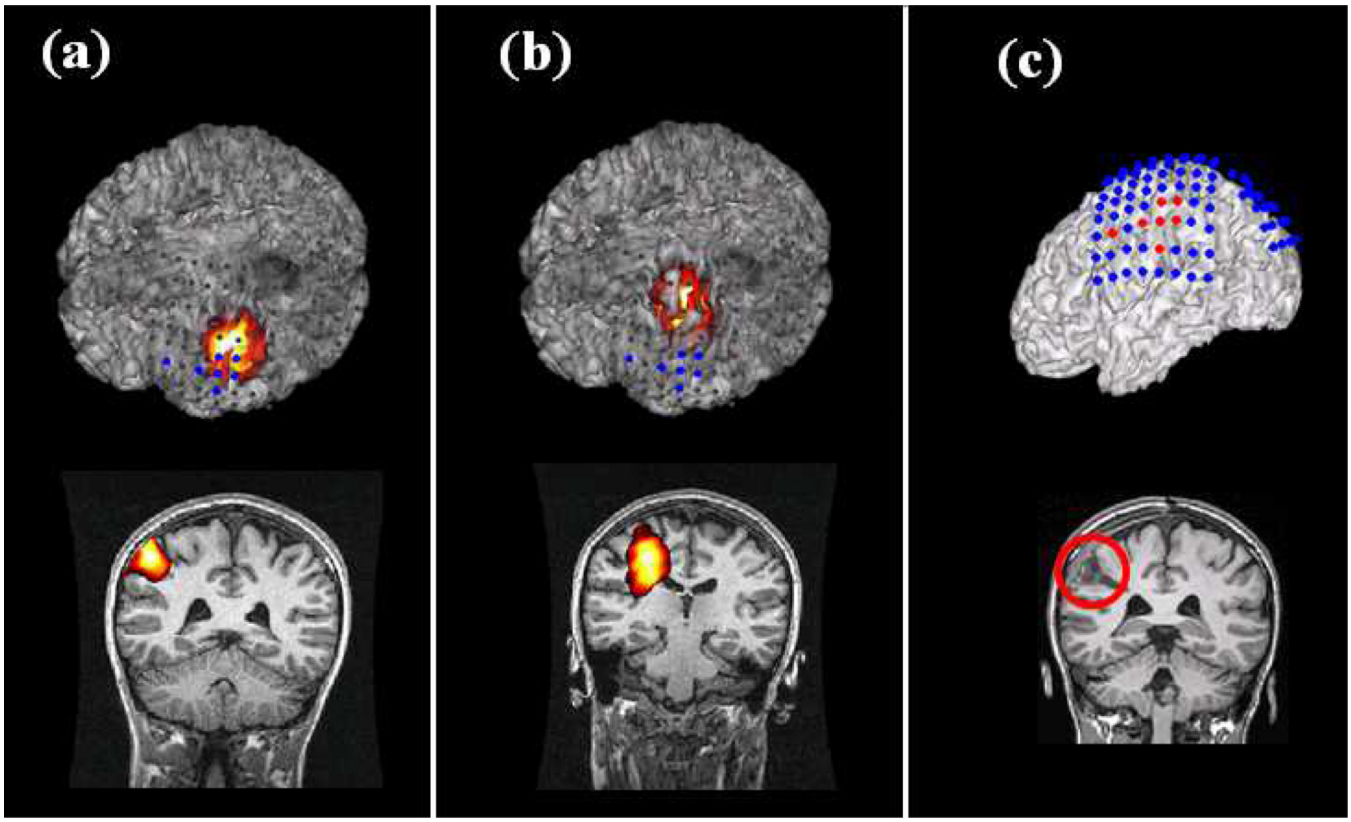

Fig. 6.

Comparison between source imaging of HF activity and interictal spike in Patient 4. (a) Source imaging results of HF activity. (b) Source imaging results of interictal spike. (c) Intracranial recording and surgical resection.

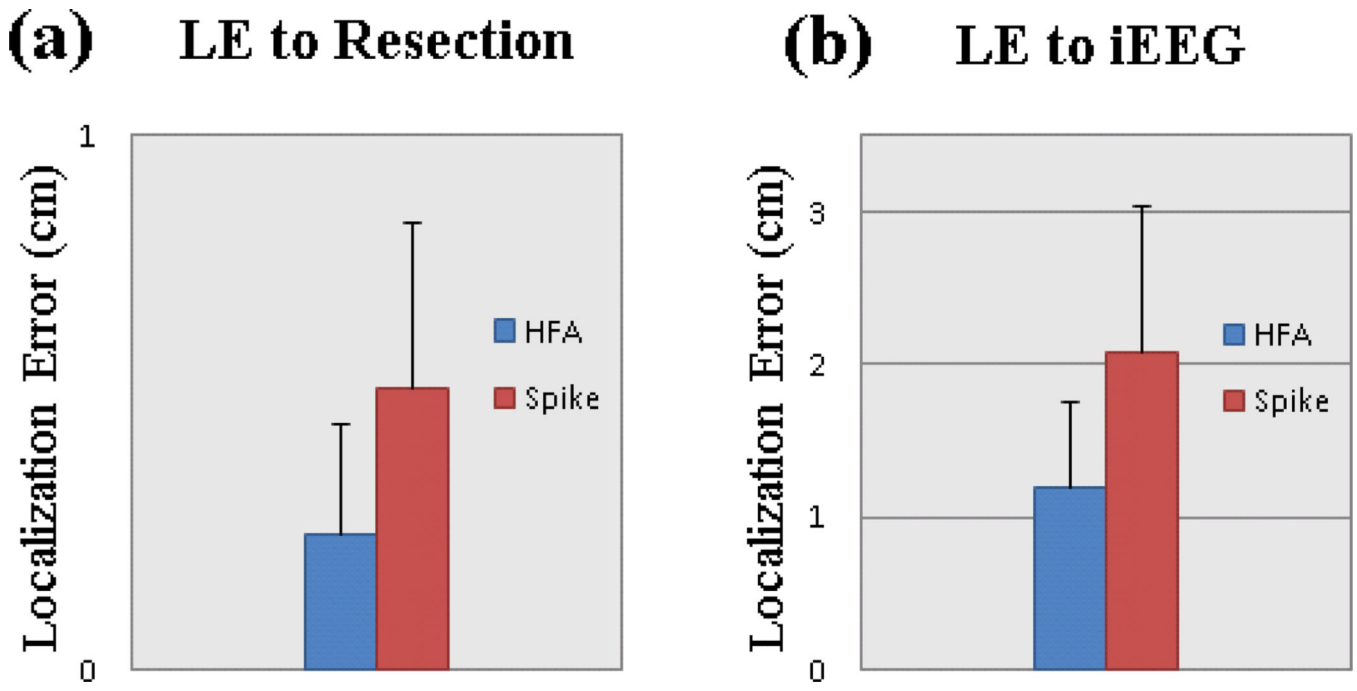

Fig. 7.

Localization error between source imaging of HF activity and spike (a) Localization error comparing with surgical resection. (b) Localization error comparing with SOZ of intracranial recording.

TABLE I

Clinical information for the patients.

ID	Age at onset	Sex	Age	Structural MRI	Surgery	Interictal EEG	Number of HF activity	Outcome	Follow-up
1	22	M	26	Normal	Right temporal lobectomy	Frequent right temporal epileptiform activity	26	ILAE-1	36 mo
2	12	F	53	Left mesial temporal sclerosis	Left temporal lobectomy	Infrequent left temporal epileptiform discharges	13	ILAE-1	18 mo
3	22	F	33	Abnormal bilateral hippocampus	Right temporal lobectomy	Frequent right temporal spikes and sharp waves	20	ILAE-1	14 mo
4	7	F	25	Normal	Left parietal focal resection	Frequent left centro-temporo-parietal spikes	29	ILAE-1	17 mo
5	14	F	26	Normal	N/A	Frequent left temporal spike and sharp waves	20	N/A	N/A

IEEE Trans Biomed Eng. Author manuscript; available in PMC 2015 June 01.